

Article

Coastal Mangrove Response to Marine Erosion: Evaluating the Impacts of Spatial Distribution and Vegetation Growth in Bangkok Bay from 1987 to 2017

Han Xiao ^{1,2,3} , Fenzhen Su ^{1,3,4,*}, Dongjie Fu ^{1,3} , Qi Wang ⁵ and Chong Huang ^{1,*}

¹ State Key Laboratory of Resources and Environmental Information System, Institute of Geographic Sciences and Natural Resources Research, Chinese Academy of Sciences, Beijing 100101, China; xiaoh@lreis.ac.cn (H.X.); fudj@lreis.ac.cn (D.F.)

² College of Resources and Environment, University of Chinese Academy of Sciences, Beijing 100049, China

³ Collaborative Innovation Center of South China Sea Studies, Nanjing University, Nanjing 210093, China

⁴ Faculty of Geomatics, Lanzhou Jiaotong University, Lanzhou 730070, China

⁵ School of Surveying and Geo-Informatics, Shandong Jianzhu University, Jinan 250101, China; wangqi19@sdjzu.edu.cn

* Correspondence: sufz@lreis.ac.cn (F.S.); huangch@lreis.ac.cn (C.H.); Tel.: +86-10-6488-8956 (F.S.); +86-10-6488-8372 (C.H.)

Received: 20 November 2019; Accepted: 3 January 2020; Published: 8 January 2020



Abstract: Long time-series monitoring of mangroves to marine erosion in the Bay of Bangkok, using Landsat data from 1987 to 2017, shows responses including landward retreat and seaward extension. Quantitative assessment of these responses with respect to spatial distribution and vegetation growth shows differing relationships depending on mangrove growth stage. Using transects perpendicular to the shoreline, we calculated the cross-shore mangrove extent (width) to represent spatial distribution, and the normalized difference vegetation index (NDVI) was used to represent vegetation growth. Correlations were then compared between mangrove seaside changes and the two parameters—mangrove width and NDVI—at yearly and 10-year scales. Both spatial distribution and vegetation growth display positive impacts on mangrove ecosystem stability: At early growth stages, mangrove stability is positively related to spatial distribution, whereas at mature growth the impact of vegetation growth is greater. Thus, we conclude that at early growth stages, planting width and area are more critical for stability, whereas for mature mangroves, management activities should focus on sustaining vegetation health and density. This study provides new rapid insights into monitoring and managing mangroves, based on analyses of parameters from historical satellite-derived information, which succinctly capture the net effect of complex environmental and human disturbances.

Keywords: spatial distribution; vegetation growth; coastal mangrove erosion; correlation coefficient

1. Introduction

Mangroves, together with their associated environments, such as rivers, deltas, offshore mudflats, and sandy habitats, provide important ecosystem services to support feeding, breeding, and nursery areas for migratory shorebirds and fish species [1,2]. A key ecological and human service from mangroves is shoreline protection through eliminating or minimizing the erosion impacts of wind and wave forces [3,4]. However, with increasing pressure from climate change and the impact of human activities, coastal mangroves are also affected by marine erosion and show different spatial and temporal responses to it [5–10]. These responses to erosion accumulate over time to affect the stability of mangrove ecosystems, as represented by its spatial coverage [11–14]. Therefore, it is

particularly important to study the relationship between marine erosion of mangroves and parameters that characterize their ability to resist marine erosion.

The phenomenon of mangrove retreat, which is well known to occur in Bangkok Bay, narrows its living space, and can lead to its disappearance [14,15]. Remote sensing datasets provide continuous temporal and spatial information on mangrove distribution, vegetation growth status, and other parameters [16], thereby providing opportunities to investigate such dynamical changes in mangrove distributions from local to global scales [9,17–22].

Mangrove erosion is generally attributed to the loss of mangrove sediment, the loss of soil microorganisms, and the lack of sediment supply. For example, previous research shows that the loss of sediment caused by sea level rise leads to the erosion and retreat of mangroves [15,23,24]. However, the health and resilience of mangrove ecosystems facing erosion is a neglected research topic. Thus, we focused on analyzing the resilience of a mangrove ecosystem using the commonly-used ecosystem evaluation parameters—spatial distribution and vegetation growth. Our study also addresses the lack of studies on the impacts changing over time, by comparing the relationship between spatial distribution and vegetation growth on mangrove retreating distance over different growth stages.

Our field survey focused on the Bay of Bangkok, where human impacts on mangroves have led to the current distribution along a narrow strip at the outermost edge of the land. To characterize this strip distribution, we assumed that the spatial distribution is represented by the cross-shore mangrove extent (width), and vegetation growth is represented by the commonly-used index normalized difference vegetation index (NDVI). Previous studies on evaluating the spatial distribution and vegetation growth of forests have mainly focused on describing temporal changes, and assessing ecosystem stability [25–29]. However, there are few studies on the impacts of spatial distribution and vegetation growth on marine erosion [30–32]; and especially, the relative importance of the parameters under different growth-stage maturity [31,32].

With this background, the study objectives were: (i) To analyze the spatial and temporal changes in mangroves distribution on the seaside in response to marine erosion, including retreating and development; (ii) to calculate and compare the relationship between mangrove width (perpendicular to the shoreline) and NDVI in cross-shore mangrove changes. This required resolving two major difficulties: Firstly, how to compute the indices quantifying mangrove width and NDVI from time-series data, whilst excluding tidal influences [19,33]; and secondly, how to quantify the relationship between the two parameters and mangrove erosion.

To study the dynamics of mangroves we used Landsat remote sensing images to quantify the spatial distribution, vegetation growth, and mangrove changes over a 30-year period. Our focus was primarily on the mangrove responses to marine erosion and whether the responses are related to spatial distribution and vegetation growth, and at what growth stage of the mangrove the relationships applied. Mangroves in Bangkok Bay have been artificially destroyed and restricted from the land side to a narrow survival strip, which in turn is subjected to erosion forces from the marine side. The remaining mangrove ecosystem there was considered endangered and fragile, requiring urgent conservation and recovery. The characteristics of the Bay of Bangkok; therefore, provide a challenging and important study area in which to examine the relationship between the stability parameters and the responses of the mangrove ecosystem to marine erosion. A further aim of the study was to contribute sound objective options for management and conservation activities for mangrove restoration and development, especially for fragile mangrove ecosystems similar to those in the Bay of Bangkok. Such studies are clearly needed to provide guidance and recommendations for the restoration of fragile mangrove ecosystems.

2. Study Area

The Bay of Bangkok (study area shown in Figure 1) is part of the Gulf of Thailand and its coastline comprises intertidal mudflats intersected by deltas and estuaries associated with the Chao Phraya River, the Tachin River, the Meckl River, and the Mamba River. Over time, dense coverages of mangroves

along its coast have been destroyed by human settlements, aquaculture, and salt pans, so that the current distribution is a narrow strip of fragile mangrove ecosystems at the outermost edge of the land [34].



Figure 1. The location and nine partitions of the study area in the Bay of Bangkok located in the northern region of the Gulf of Thailand.

Through two interviews with the fish pond owner of what was once an original mangrove growing area, we were able to determine the following history of mangrove distributions and changes. With the population increasing, from 1961 the local government allowed private occupation and development of mangroves. Since the 1960s, mangroves in the Bay of Bangkok have experienced private and governmental deforestation and occupation [35], including aquaculture, shrimp farming, salt pans, and expansion of urban areas. The destruction was particularly serious on the coast from Samut Sakhon province to Chachoengsao province, where mangrove coverage was reduced to a minimum, with information showing that there was only 1,047,390 rai (A rai is a unit of area equal to 1600 square meters.) left in the Bay of Bangkok area around 1996. Since the 1990s, aquaculture has become less profitable than in the past due to damage to the coastal environment. Moreover, fluctuations in the price of aquaculture products in the market have led to the abandonment of many fish ponds. The local government began restoring mangroves around 2000 so that mangroves began to gradually enter the recovery phase.

3. Materials and Methods

3.1. Field Measurements and Investigations in the Study Area

Field investigations were carried out in the Bay of Bangkok during September 2018 over the mangrove protection areas and the fish pond areas adjacent to the mangroves. Data collected included locations of verification points, and interviews were conducted to determine the history of mangrove coverage and changes in the area including human disturbances. In the study area, the spectral difference between water body (including pond, salt field, and sea water) and mangrove is significant, while the spectral difference between mangrove and other vegetation is small, thus requiring field verification of the vegetation classifications. The main aim of the field investigations was determining the border between mangrove and other vegetation. The Global Positioning System (GPS) and Open

Street Map (OSM) Tracker were used to record the position and land cover properties at the 38 field verification points, as shown in Figure 1.

3.2. Satellite Data Processing and Mangrove Mapping

For time-series analysis of the dynamic changes in mangroves, we used Landsat due to the availability of a long-term sequence of continuous data [36]. We used the 30-year Landsat collection [37] including sensors of TM\ETM+\OLI. The U.S. Geological Survey provided a Landsat archive, reorganized as a tiered collection structure, to ensure that the Landsat Level-1 products provide a consistently accessible stack of known data quality suitable for time-series analyses and data stacking. Data from 1987 to 2017 (except for 2012 due to the lack of data) of Landsat yearly data were processed via Google Earth Engine (GEE) [38].

Taking 2017 as an example, we generated 394 sample points in the study area, including 38 field collection points (as shown in Figure 1). Because of extensive changes in the mangroves over the 30 years, we used the sample points of 2017 as a standard, and changed the sample points according to the image year-by-year, before finally generating the 1987–2017 sample points. The sample points were divided into four classes (mangroves, water, bare land, and other vegetation), and the classification and counts in each class are shown in Table 1 below. We randomly selected 75% of these points in the sample point dataset as training points and 25% as verification points. In addition to the spectral bands of Landsat data (blue to Swir2), to distinguish between mangrove and other vegetation, three types of vegetation indexes were used: NDVI, enhanced vegetation index (EVI), and soil-adjusted vegetation index (SAVI). For differentiating between mangroves and water bodies, the normalized difference water index (NDWI) was used in the classification. Finally, considering that mangroves grow in low-lying areas near the sea, elevation collected from SRTM Digital Elevation Data [39] was used.

Table 1. Counts of the sample points of the Landsat image of 2017 used for four-class classification.

Class	Mangrove	Water	Bare Land	Other Vegetation
Counts of Sample points	108	77	67	42
Counts for training	81	58	50	31
Counts for verification	27	19	17	11

We mentioned in the introduction that effective mangrove change detection over long time-series requires removal of the tide influence, or by aggregating over periods much longer than the tidal period. To resolve the problem, we extracted the mangrove information from 1987 to 2017 using GEE according to the following process:

- (i) Generate yearly fusion images, which were used to classify mangroves of each year, by taking the median value of the annual Landsat images with less than 30% cloud in the GEE dataset;
- (ii) Use random forest to classify the four classes using the following bands: Blue, Green, Red, Nir, Swir1, Swir2, NDVI, EVI, SAVI, NDWI, together with Elevation;
- (iii) Verify the mangrove classification results with the field observations at the sample points. Furthermore, the proportion of common area of mangrove classification results of two published land cover or mangrove distribution datasets was calculated to verify the reliability (as shown in Table 2).

Table 2. The accuracy assessment.

Data Set for Verification	Mangrove Classification Result	Accuracy
Verification points (25% of total sample points)	Results from 1987–2017	90.91%–96.24%
Data Set for Verification	Mangrove Classification Result	Proportion of Common Area
Mekong region Land cover 2000–2017 [40]	Results from 2000–2017	80.36%–88.21%
Global mangrove forests 2000 [41]	Result of 2000	87.39%

3.3. Relationship Resolution

The relationship between mangrove stability and response to marine erosion is confounded by a number of factors, such as the direction of the coast relative to wave direction, coastline geomorphology, and sediment substrate [42]. At a smaller scale of mangrove patches, there are also spatial differences in marine erosion. Thus, it is difficult to establish and deterministically model the relationship between variables governing responses to marine erosion. For this study, we chose to investigate statistical correlations between parameters and yearly erosion distance, in order to provide a rapid and objective method from which we can derive abstract quantitative methods and clear association rules [43].

The flow chart, shown in Figure 2, graphically summarizes our method to quantify the relationship between mangrove responses to marine erosion, spatial distribution, and vegetation growth.

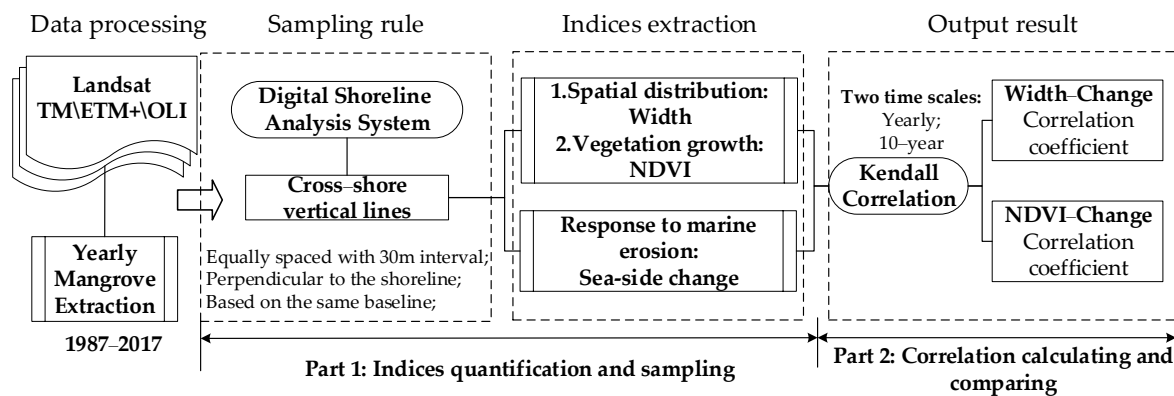


Figure 2. A flow chart describing the data and methodology.

3.3.1. Sampling Rule and Indices Extraction

In order to account for changes in the intensity of marine erosion as a function of the bay's direction, the study shoreline was selectively divided into nine partitions based on shoreline direction and shape, the natural division caused by estuaries, and the observed mangrove distribution. These divisions of the study area are shown in Figure 1.

The methodology we employed was based on the following ideas:

(i) Simplify the quantification method: To account for the directionality of mangrove erosion relative to the coast, we used equally spaced lines perpendicular to the shoreline to provide transect statistics for the sampled mangrove [44]. To ensure transects sampled mangrove for 30 years, the baseline was established offshore at an average distance of 1.27 km. Based on the same baseline, transects with a length of 5 km were established with samples at 30 m intervals along the transect. The schematic diagram in Figure 3 shows how the transects were established.

(ii) Control the variables spatially: Regional variations in the propensity of marine erosion were controlled by dividing the study area into nine units/sub-regions (Zone 1 to Zone 9, shown in Figure 1) in order to control marine erosion factors such as current, sea breeze, soil quality, and sea level rise in each unit. We used these units as the spatial basis to explore the different sub-regional responses of mangroves, and performed a 30-year time-series analysis of the average width, NDVI, and seaside values from the nine partitions.

Special considerations were required to define the following key parameters of this study: The mangrove response to mangrove erosion; the spatial distribution of mangrove ecosystem; and vegetation growth. First of all, the change of mangrove on the seaside, including retreat and growth (positive values represent growth seaward, and negative values represent retreat landward), were measured to represent the response to marine erosion. Considering the narrow strip distribution of mangroves in the study area, cross-shore mangrove extent was used to define mangrove spatial distribution characteristics, and NDVI was used for mangrove growth characteristics. Thus, the values sampled by the sampling lines included: The long-term sequence of mangrove change on the seaside;

cross-shore mangrove extent; mean NDVI of each line, which represent mangrove response to marine erosion; the spatial distribution; and vegetation growth, respectively. The detailed descriptions of each index are provided in Table 3.

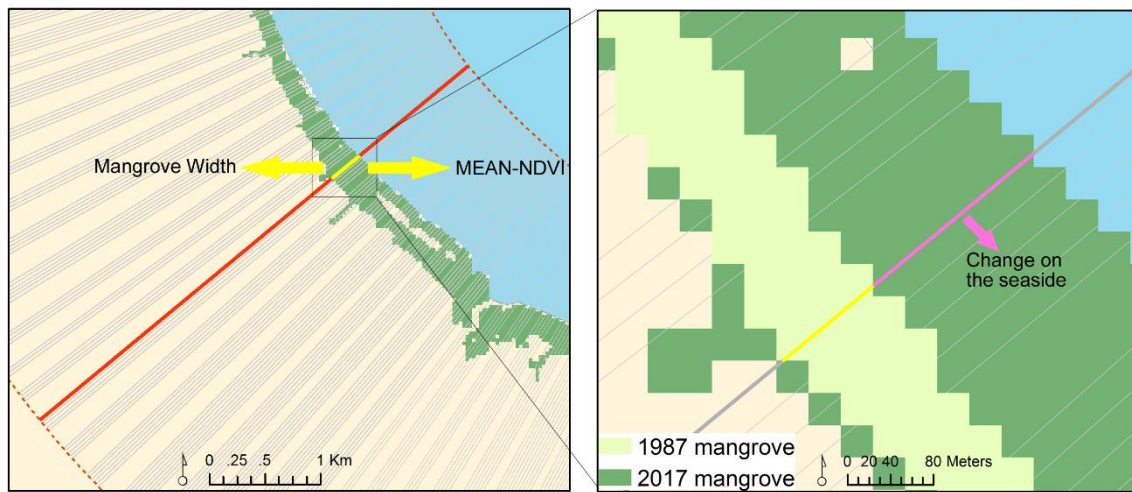


Figure 3. Schematic showing the mangrove transect sampling line established from an offshore baseline (see text for definition) and extending roughly perpendicular to the coast for a length of 5 km, with samples of mangrove width and normalized difference vegetation index (NDVI) taken at 30 m intervals along the transect.

Table 3. Description and formulas for the parameters and indices used in the calculations in the paper.

Parameter	Indices	Calculation Formula	Description
Spatial distribution	Cross-shore mangrove extent	W_k	The length of the mangrove width along the sample line.
Vegetation growth	NDVI	$\frac{1}{n_k} \sum_i^{n_k} NDVI_i$	The mean NDVI of the mangrove pixels (n_k pixels) along the sample line.
Response to marine erosion (RME)	Change on the seaside	$-(L_{y_2} - L_{y_1})$	The difference between the length of mangrove in the first year (L_{y_1}) and the length at the end of the relevant year (L_{y_2});

where i = cell number, k = transect number, and y = year; $y_2 > y_1$.

3.3.2. Long Time-Series-Based Relational Analysis Method

1. Time-series regression of yearly width and NDVI changes from 1987 to 2017: Time-series based on Landsat images provide an opportunity to observe and characterize relative trends in disturbance and resilience at a regional scale, by disturbance type and ecozone, and at a spatial level that is relevant to both forest management and science [45]. The interpretation of geographical phenomena at different time scales can represent procedural and phased characteristics [46]. In order to reveal the trend of mangrove width, NDVI, and changes on the seaside over 30 years, a yearly-based Loess regression analysis was used to examine temporal variations from 1987–2017 of mangrove width, NDVI, and responses to marine erosion in the nine mangrove ecosystems. Loess regression is a nonparametric technique that uses local weighted regression to fit a smooth curve, which can reveal trends and cycles in data [47].

2. Kendall correlation analysis at yearly and 10-year scale: The relationship of mangrove *Width-Change* and *NDVI-Change* was computed using the Kendall rank correlation coefficient (often called Kendall's τ or tau)—a non-parametric test which measures the strength of the relationship between two variables [48]. In calculating the correlations, we used rank correlations based on Kendall's tau, which is often said to be robust in the sense of capturing patterns and being resistant to outlying observations [49]. The tau correlation coefficient (tau-CC) of *Width-Change* and *NDVI-Change* were

calculated at yearly and 10-year scales in order to compare the relationship between parameters and marine erosion responses in different regions and growth stages.

4. Results

4.1. Dynamics of Coastal Mangrove Change Across 30 Years

We began the analysis by comparing the overall changes of mangroves between 1987 and 2017 across the nine sub-regions. Our field observations revealed that the distribution of mangrove patches were small and strip-type. This led us to use spatial and temporal aggregation approaches in order to study local and regional changes. Local changes were estimated by the width and NDVI parameters along transects (Figure 4), and regional changes were examined from the trends of mangrove change from 1987 to 2017 for each partition (Figure 5). These analyses provided both regional and fine-scale understanding of the mangrove changes across the bay and across time.

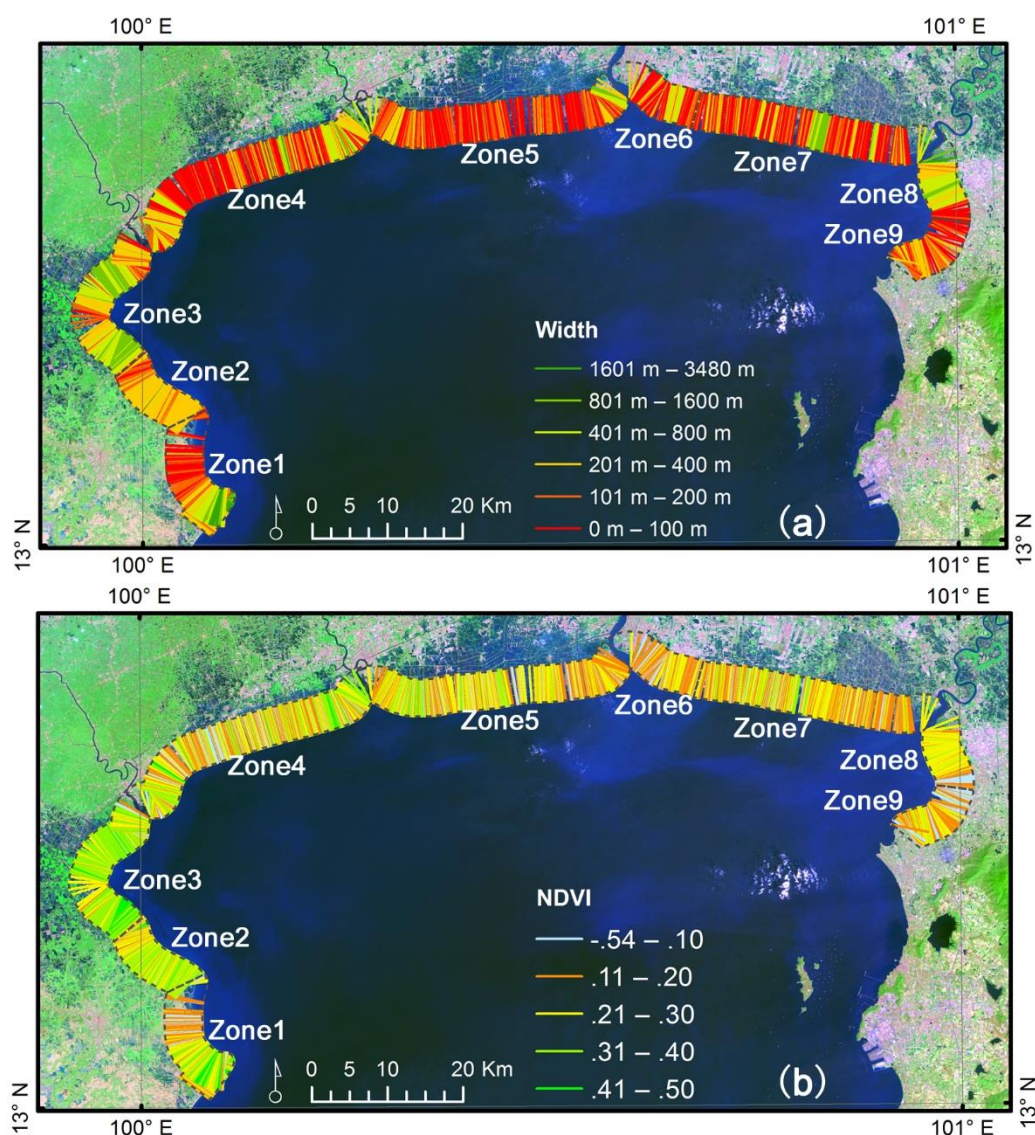


Figure 4. Transect lines, of 5 km length, used to calculate mangrove width and NDVI status in 2017. (a) Shows the transect-based spatial distribution of mangrove width; (b) shows the same distribution for NDVI; the background Landsat image was obtained on 3 February 2018.

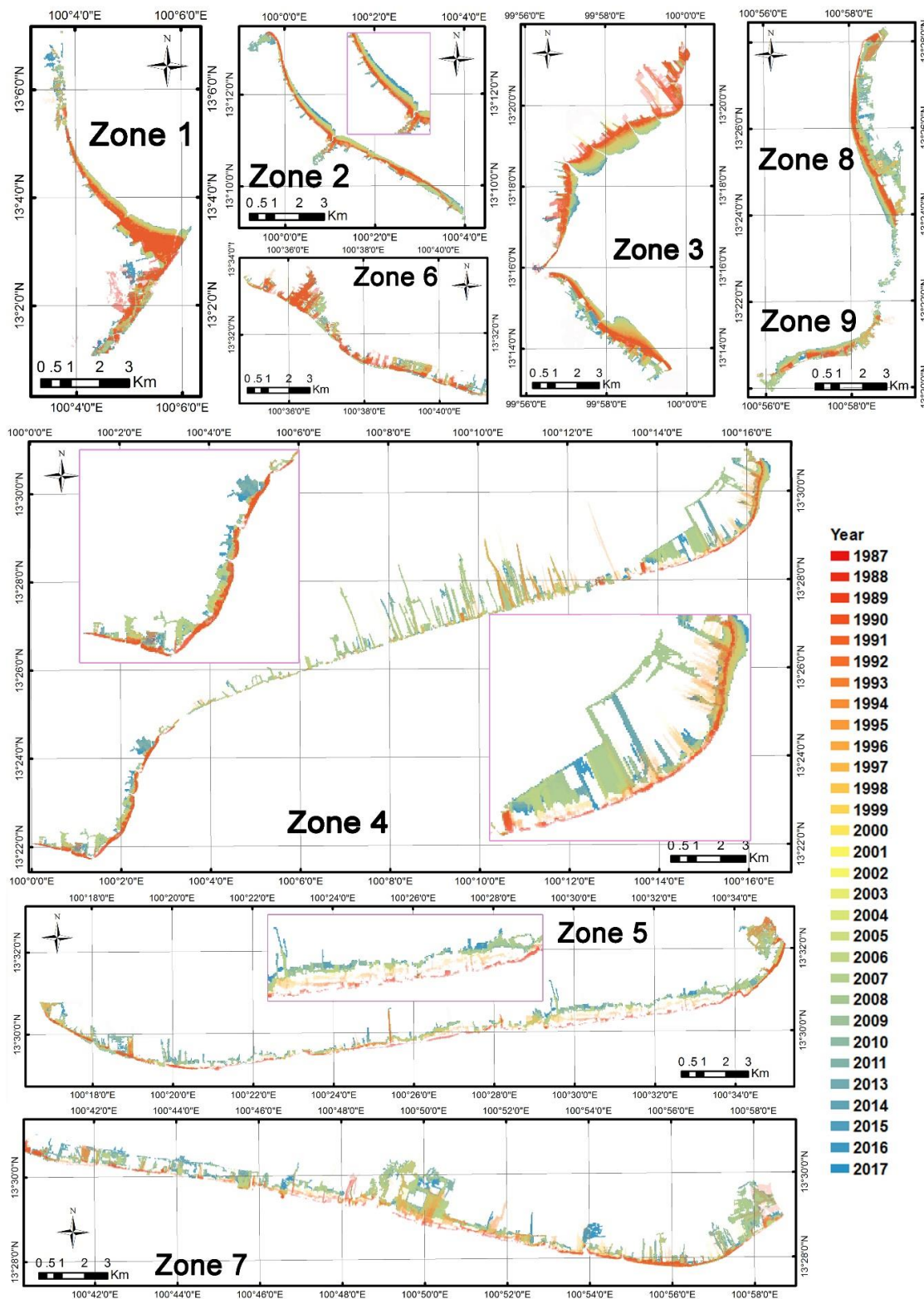


Figure 5. Distribution along the coast of mangrove in each of the study regions from 1987 to 2017.

Figures 4 and 5 allows us to compare mangrove width and NDVI status in 2017 and the changes over 30 years. Mangroves of the west coast of the Bay of Bangkok were relatively wide and had high NDVI, with width varying between 400–800 and 800–1600 m and NDVI above 0.3; these values indicate mangroves in a growth situation. Newly-grown mangroves were most widely distributed along the east coast, and mangroves here were wide but with a low NDVI. Mangroves growing in the north

bank of the Bay of Bangkok, close to the human settlement environment, were narrow and of low NDVI, except for mangroves distributed around the estuary. The width values in this area were mostly distributed within 0–200 m, with NDVI of 0.1–0.3.

The change to the seaside in the aggregate of coastal mangroves between 1987 to 2017 in each of the regions (as defined in Table 3) is summarized in Table 4, which shows that the order of change is Zone 3 > Zone 1 > Zone 2 > Zone 8 > Zone 9, with the largest value in Zone 3 which grows 317.1 m seaward. The order of retreating was Zone 7 > Zone 5 > Zone 4 > Zone 6, with the largest retreating value in Zone 7, which retreats 142.8 m landward.

Table 4. Mangrove change on the seaside from 1987 to 2017 of coastal mangroves in the nine zones.

Region	Zone 1	Zone 2	Zone 3	Zone 4	Zone 5	Zone 6	Zone 7	Zone 8	Zone 9
Change (m)	166.2	115.5	317.1	−36.0	−140.1	−31.1	−142.8	108.0	62.7

The maps of coastal mangrove distribution in Figure 5 display an obvious spatial differentiation of mangrove response to marine erosion in the nine partitions: Mangroves retreated in three zones in the northern coast of the Bay of Bangkok (Zone 4, Zone 5, and Zone 7), while growth occurred in three zones of the west coast (Zone 1, Zone 2, Zone 3) and in two zones of the east coast (Zone 8 and Zone 9). Mangrove retreats were, in general, landward, apart from mangroves near the estuaries, which retreated to a lesser extent. Distribution and trends of NDVI show five zones where growth occurred (Zone 1–3 and Zone 8–9), and NDVI growth was relatively stable internally. Zones where retreat occurred were low in NDVI status, regardless of whether it was 1987 or 2017.

Comparative analysis of trends within and between the regions were analyzed from annual changes across 1987 to 2017 of three Loess-regression trends: (1) Change of mangrove boundary at the seaside; (2) width; and (3) NDVI. The trends of the width and NDVI are displayed in Figure 6, and the trend of coastal mangrove change on the seaside are shown in Figure 7. Regressions were computed across the 30 years between the annual change of mangroves on the seaside (in meters), the annual mangrove width (in meters), and the annual mangrove NDVI.

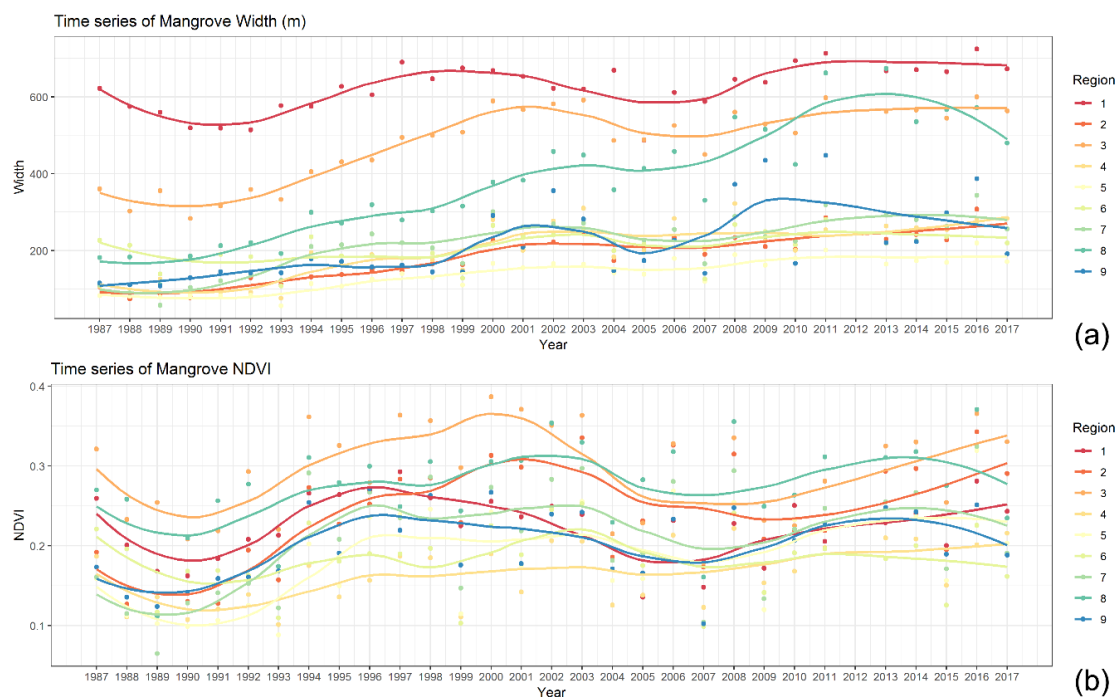


Figure 6. Yearly time-series of mangrove width and NDVI. (a) The trend of mangrove width in nine regions from 1987 to 2017; (b) the trend of mangrove NDVI in nine regions from 1987 to 2017.

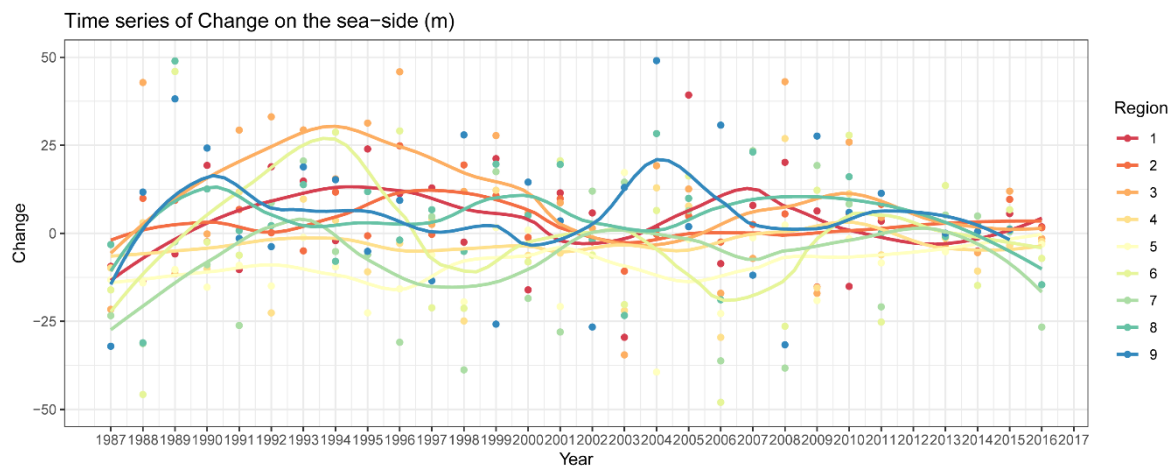


Figure 7. Annual change of coastal mangrove on the seaside from 1987 to 2017. Positive numbers (in meters) imply mangroves extending seaward, while negative numbers imply a retreat (contraction) landward. Zones and their numbering are identified in Figure 1.

The 30-year time-series of width and NDVI exhibited the following general phenomena: (1) The width of the nine regions increased from 1987 to 2017, rates of which slow down after 2003, and the largest width increase was in Zone 8; (2) the width of three regions retreated (Zones 4, 5, and 7) and they were all of low widths as well (note that the mangroves of the three retreated regions retreated in the direction from sea to land); (3) the trend of the NDVI curve of mangroves in all the study regions displayed an upward trend, and changes between regions were broadly consistent in time, except after 2015; (4) NDVI displayed consistent growth periods within 1993–2005 and 2012–2015, and two distinct troughs in 1990 and 2007. The three retreating regions experienced NDVI increases but poor growth.

Additional observations from Figure 7 are that the trend across nine regions can be divided into rapid growth phases in 1990–1997 and in 2004–2008, and slow growth or retreating phases in 1987–1989 and 2000–2003. While the retreating areas (Zones 4, 5, and 7) showed significant retreat in most years, the most significant retreats occurred in 2001–2009. After 2010, the retreating reduced in Zones 4 and 5. In 2015–2017, Zone 4 extended by growing out to the sea. Since 1990, mangroves in the growing regions (Zones 1, 2, 3, 8, and 9) began to recover and extend out to the sea. After 2004, the rates of growth slowed in the five regions, and some retreated slightly. The largest retreat occurred in Zone 8, which retreated 78 m in 2009.

In summary, the different mangrove responses to marine erosion and its impact on width and NDVI across 30 years showed that:

(i) Mangroves in Zones 1, 2, 3, 8, and 9 grew at a constant stable rate out to the sea; the mangroves in Zones 4, 5, and 7 retreated landward, with narrow width and poor growth state;

(ii) The broad trends of width and NDVI change across the nine regions showed a consistent but fluctuating rise. For growing regions, mangroves with wider extent and higher NDVI show more significant growth out to the sea. For retreating regions, mangroves with wider extent and higher NDVI retreated shorter distances;

(iii) The retreat rates of regions 4 and 5 gradually stabilized after 2011, with width and NDVI increasing, while region 4 stopped retreating in 2015–2017 and showed seaward growth.

4.2. Relationship between Width-Change and NDVI-Change

The 30-year time-series mangrove change in the Bay of Bangkok showed different responses to marine erosion, represented by periods of growth and retreat. In this section, we analyze those changes in relation to changes in mangrove width and NDVI by computing the Kendall-tau correlation coefficients (tau-CCs) between the *Width-Change* and *NDVI-Change*. The characteristics of the relationship above

were analyzed at short and long-time scales corresponding to yearly and 10-year scales, respectively. The tau-CCs were computed between mangrove width at those two time scales, and similarly for NDVI.

4.2.1. Correlations at the Yearly Scale

The annual tau-CCs, displayed in the heat map in Figure 8, shows that annual retreats or growth were small—as indicated by low values for tau-CCs.

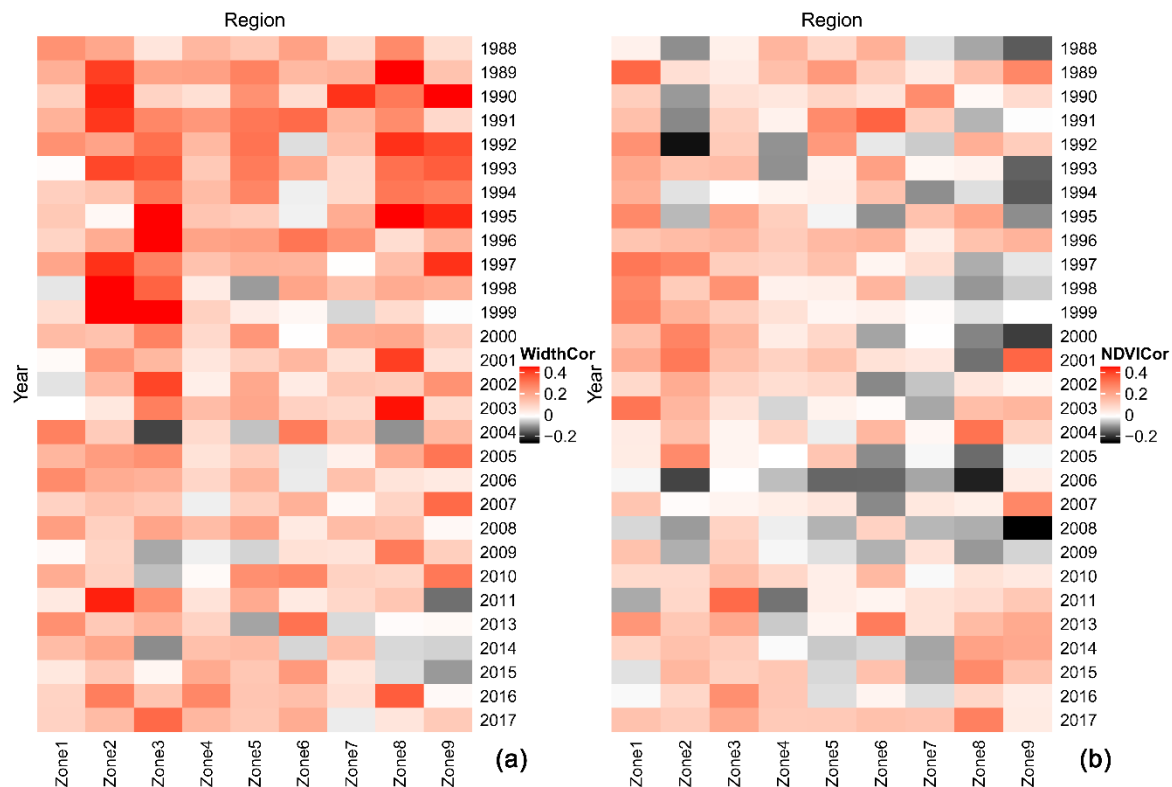


Figure 8. The thermogram of Kendall tau-CC (correlation coefficient, CC) results for *Width-Change* (a) and *NDVI-Change* (b) at the yearly scale. Positive values (warm tones) represent similarity in the profile of ranked values, while negative values (gray tones) indicate a disparity in the rank profile. White values indicate irrelevant results for the correlations. The color depth represents the level of the correlation coefficient.

Significant patterns from Figure 8 of the trends in yearly tau-CCs of *Width-Change* and *NDVI-Change* in response to marine erosion are as follows:

(i) tau-CCs: Overall, the tau-CCs for width are greater than those for NDVI, implying that the pattern of yearly changes in width are more consistent than those for NDVI; possibly also implying that changes in NDVI are more dynamic at yearly time-scales and less consistent;

(ii) Width pattern: Zone 2 > Zone 3 > Zone 8 > Zone 9 > Zone 5 > Zone 1 > Zone 6 > Zone 4 > Zone 7, with the early stage (1988–2003) values being greater than those for the current stage (2004–2017);

(iii) NDVI pattern: Zone 1 > Zone 3 > Zone 2 > Zone 8 \approx Zone 9 > Zone 6 > Zone 5 > Zone 4 > Zone 7, with rapid growth stages in (1993–2004) and (2013–2017) greater than the poor growth stages in (1989–1992) and (2005–2009).

4.2.2. Correlations at the 10-Year Scale

Three periods were used to compute the correlations at the 10-year time scale: 1987–1997, 1997–2007, and 2007–2017. For these periods, tau-CCs were calculated for width and NDVI. Correlations between *Width-Change* and *NDVI-change* for the three periods are listed in Table 5.

According to the annual mangrove changes displayed in 3.1.2 (Figure 6a), the change rates in the nine regions showed that 1987–1997 > 2007–2017 > 1997–2007. By comparison, the tau-CCs of the three periods (shown in Table 5) revealed the following phenomena:

(i) As per the yearly analysis, the positive impacts of width on mangrove stability were greater than that of NDVI;

(ii) For regions with large mangrove patches, NDVI had a greater influence than for other regions. For example, for Zone 1 with the largest mangrove patch and width value, the positive impact of width was ranked fourth out of the nine regions, while the positive impact of NDVI was ranked first;

(iii) For the newly-grown mangrove regions, such as zones 2, 3, 8, 9, the impact of width was much larger than the influence of NDVI;

(iv) For areas with smaller width and NDVI, such as Zone 4 and Zone 7, the tau-CCs were extremely low;

(v) For the growing stages (1987–1997) and (2007–2017), the positive impacts of width and NDVI were higher compared to the poor growth stage (1997–2007).

Table 5. The tau-CC results of *Width-Change* and *NDVI-Change* using a 10-year aggregation scale. Significance levels for the correlations are shown below the Table.

Width	Zone 1	Zone 2	Zone 3	Zone 4	Zone 5	Zone 6	Zone 7	Zone 8	Zone 9
1987–1997	0.36 ***	0.40 ***	0.59 ***	0.41 ***	0.16 **	0.43 ***	−0.02	0.29 ***	0.50 ***
1997–2007	0.12 ***	0.25 ***	0.44 ***	−0.03	0.17 **	−0.04	−0.01	0.15 **	0.25 ***
2007–2017	0.43 ***	0.27 ***	0.23 ***	0.00	0.20 ***	0.46 ***	−0.03	0.27 ***	0.38 ***
NDVI	Zone 1	Zone 2	Zone 3	Zone 4	Zone 5	Zone 6	Zone 7	Zone 8	Zone 9
1987–1997	0.38 ***	0.24 ***	0.36 ***	0.21 ***	0.07 *	0.28 ***	−0.03	0.02	0.36 ***
1997–2007	0.14 ***	0.31 ***	0.12 **	−0.04	0.19 ***	−0.12 **	−0.02	0.07 *	0.03
2007–2017	0.29 ***	0.21 **	0.21 **	0.05	0.10 *	0.38 ***	0.06	0.21 ***	0.24 ***

*** $p < 0.001$, ** $p < 0.01$, * $p < 0.05$, $p < 1$.

5. Discussion

5.1. Quantification Method for Long-Term Analyses

Our study focused on using satellite remote sensing in order to provide rapid and relevant information on different recovery and protection measures during different future stages of mangrove growth. Reviews of mangrove classification suggest that mangroves grow in tropical and subtropical intertidal zones where it is difficult to avoid errors caused by cloudy images and tidal flooding [19]. In addition, NDVI of mangrove, as a correlation factor of mangrove change calculated in our study, also has seasonal differences. Thus, long-term mangrove classification and impact comparisons requires removal of the uncertainty from tidal influence and NDVI seasonal changes.

In this study, the tidal influences were eliminated by aggregating and median-filtering Landsat data to annual images. We calculated the median value of all bands for the whole year of the Landsat collection Level-1 images by using only images with under 30% cloud cover. Mangroves were classified using the yearly images. At the same time, the NDVI from the yearly images was used, thus avoiding problems from seasonal changes.

5.2. The Impacts of Spatial Distribution and Vegetation Growth in the Various Growing Stages

In this study, we chose the yearly scale to display trends and relationships at short time scales and a 10-year scale for longer-term changes. Yearly changes showed low correlations, and we used the 10-year analyses to highlight the relationships between spatial distribution and vegetation growth in different long-term stages. Both the yearly and 10-year tau-CC results revealed that the positive effects of width were greater than those for NDVI.

The long-term sequence quantification showed that there were differences in growth and relationships between the mangrove parameters. The positive impacts of mangrove spatial distribution and vegetation growth status on stability varied in the different growing stages and zones: Zone 2 and Zone 3 were regions where mangrove width increased the most, and Zone 8 and Zone 9 had a large number of young mangroves with low NDVI. The relationship between width and response was more obvious during the high-speed recovery and development phase, 1987–2000, but that relationship declined with time. Hence, as mangrove width increased, in other words as mangroves grew in time, the positive effect of width decreased. Zone 1 had the widest mangrove forest of the nine regions, with the highest NDVI and second highest mangrove growth rate, but the positive effect of width was weak at the sixth rank. These results imply that, during the early growth stage, the width of the original mangrove ecosystem had a strong effect on stability, as opposed to NDVI.

The tau-CCs of NDVI-change (see Figure 8 and Table 5) and the 30-year NDVI trends (see Figure 6), show that strong growth of NDVI is consistent with high initial NDVI values. This implies that vegetation biomass in the original mangrove forest ecosystem displayed a strong positive impact on its later development when NDVI increases. For example, in Zone 1 mangroves grew significantly and had the highest NDVI. At the same time, the positive impact of NDVI was the highest among the nine regions. Additionally, Zones 2, 3, 4, 5, and 6 all had high tau-CCs during years with higher NDVI (1996–2003 and 2013–2017). In Zones 8 and 9, mangrove recovery was lagging behind Zones 2 and 3, reflected in the very low positive, and negative, impact of NDVI in the early stage of mangrove development. As the width of mangrove in these two regions gradually increased, the positive effects of NDVI appeared after 2010.

In summary, mangrove width rather than NDVI appeared to offer greater resistance to marine erosion. At the early growth stage of mangroves, width impacts were particularly prominent. As mangrove width increased, at a certain width with a high NDVI value, positive impacts of vegetation growth status, like health and density, appeared.

Mangrove ecosystems are a complex sea–land link system, and future research effort is needed to verify and extend the findings of this study by using multi-source data, multiple indicators, and models. For example, the stability of the mangrove ecosystem is not only related to the spatial distribution and vegetation growth parameters but also to its environmental factors such as climate, tidal fluctuation, sediment, and wave energy [50].

6. Conclusions

Our investigation and analyses of mangrove dynamics in the Bay of Bangkok show that two parameters most commonly used in forest ecosystem evaluation—spatial distribution and vegetation growth—affect mangrove dynamics differently for different growing stages. The main conclusions of the study are as follows:

Broadly, both spatial distribution and vegetation growth of mangroves display positive impacts on their defensive ability to marine erosion.

Mangroves with small width and low NDVI appear to continuously retreat landward as part of a coastal squeeze phenomenon, while mangroves of wide width and high NDVI perform stable or seaward extensions.

The positive effect of the spatial distribution was greater than vegetation growth, especially for mangroves at an early growth stage. However, as mangroves mature and grow, the vegetation growth status becomes more relevant than spatial distribution.

Thus, overall, we find that the impact of spatial distribution is higher at the early growing stage, while the impact of vegetation growth is higher at mature growing stages. The implication is that at the initial stage of mangrove restoration or cultivation, planting should focus on width and area, while for mature growth stages, attention should focus on increasing the vegetation health and density to maintain ecosystem stability.

Our research, which uses readily available remotely sensed images, provides objective guidance on planting structure and coverage relevant to the management, restoration, and development of mangroves, especially for fragile mangrove ecosystems that are in need of urgent restoration in the Bay of Bangkok.

In future, we aim to extend the research to explore the relationship between environmental factors and parameters computed from remotely sensed images. Such studies are needed in order to develop predictive models of how mangrove extent and health will be affected by changes in environmental factors that affect marine erosion. A further aim of future research is to use high-resolution data to separate mangrove tree species in order to understand species-related responses to changes in the environment.

Author Contributions: All authors contributed to this manuscript: F.S. and C.H. conceived the research and collected all the data; F.S., H.X., and C.H. designed the experiment and drafted the manuscript; C.H., D.F., and Q.W. provided help with the language and reviewed the manuscript. All authors have read and agreed to the published version of the manuscript.

Funding: This research received no external funding.

Acknowledgments: This work was supported by the Strategic Priority Research Program of the National Natural Science Foundation of China (Grant Number: 41421001) and the Chinese Academy of Sciences (Grant Number: XDA19060300).

Conflicts of Interest: The authors declare no conflicts of interest.

References

1. Atwood, T.B.; Connolly, R.M.; Almahasheer, H.; Carnell, P.E.; Duarte, C.M.; Ewers Lewis, C.J.; Irigoien, X.; Kelleway, J.J.; Lavery, P.S.; Macreadie, P.I.; et al. Global patterns in mangrove soil carbon stocks and losses. *Nat. Clim. Chang.* **2017**, *7*, 523–528. [[CrossRef](#)]
2. Curnick, D.J.; Pettoirelli, N.; Amir, A.A.; Balke, T.; Barbier, E.B.; Crooks, S.; Dahdouh-Guebas, F.; Duncan, C.; Endsor, C.; Friess, D.A.; et al. The value of small mangrove patches. *Science* **2019**, *363*, 239. [[PubMed](#)]
3. Alongi, D.M. Mangrove forests: Resilience, protection from tsunamis, and responses to global climate change. *Estuar. Coast. Shelf Sci.* **2008**, *76*, 1–13. [[CrossRef](#)]
4. McIvor, A.; Möller, I.; Spencer, T.; Spalding, M. *Reduction of Wind and Swell Waves by Mangroves. Natural Coastal Protection Series: Report 1*; Cambridge Coastal Research Unit Working Paper 40; The Nature Conservancy and Wetlands International: London, UK, 2012; ISSN 2050-7941.
5. Danielsen, F.; Sorensen, M.K.; Olwig, M.F.; Selvam, V.; Parish, F.; Burgess, N.D.; Hiraishi, T.; Karunakaran, V.M.; Rasmussen, M.S.; Hansen, L.B.; et al. The asian tsunami: A protective role for coastal vegetation. *Science* **2005**, *310*, 643. [[CrossRef](#)]
6. Gracia, A.; Rangel-Buitrago, N.; Oakley, J.A.; Williams, A.T. Use of ecosystems in coastal erosion management. *Ocean Coast. Manag.* **2018**, *156*, 277–289. [[CrossRef](#)]
7. Cai, F.; Su, X.; Liu, J.; Li, B.; Lei, G. Coastal erosion in China under the condition of global climate change and measures for its prevention. *Prog. Nat. Sci.* **2009**, *19*, 415–426. [[CrossRef](#)]
8. Barbier, E.B. The protective service of mangrove ecosystems: A review of valuation methods. *Mar. Pollut. Bull.* **2016**, *109*, 676–681. [[CrossRef](#)]
9. Giri, C.; Long, J.; Abbas, S.; Murali, R.M.; Qamer, F.M.; Pengra, B.; Thau, D. Distribution and dynamics of mangrove forests of South Asia. *J. Environ. Manag.* **2015**, *148*, 101–111. [[CrossRef](#)]
10. Godoy, M.D.; de Lacerda, L.D. Mangroves response to climate change: A review of recent findings on mangrove extension and distribution. *An. Acad. Bras. Ciências* **2015**, *87*, 651–667. [[CrossRef](#)]
11. Woodroffe, C.D. Response of tide-dominated mangrove shorelines in northern Australia to anticipated sea-level rise. *Earth Surf. Process. Landf.* **1995**, *20*, 65–85. [[CrossRef](#)]
12. Jallow, B.P.; Barrow, M.K.A.; Leatherman, S.P. Vulnerability of the coastal zone of the gambia to sea level rise and development of response strategies and adaptation options. *Clim. Res.* **1996**, *6*, 165–177. [[CrossRef](#)]
13. Gilman, E.; Ellison, J.; Coleman, R. Assessment of mangrove response to projected relative sea-level rise and recent historical reconstruction of shoreline position. *Environ. Monit. Assess.* **2007**, *124*, 105–130. [[CrossRef](#)] [[PubMed](#)]

14. Woodroffe, C.D. Mangrove response to sea level rise: Palaeoecological insights from macrotidal systems in northern Australia. *Mar. Freshw. Res.* **2018**, *69*, 917–932. [[CrossRef](#)]
15. Schuerch, M.; Spencer, T.; Temmerman, S.; Kirwan, M.L.; Wolff, C.; Lincke, D.; McOwen, C.J.; Pickering, M.D.; Reef, R.; Vafeidis, A.T.; et al. Future response of global coastal wetlands to sea-level rise. *Nature* **2018**, *561*, 231–234. [[CrossRef](#)]
16. Kuenzer, C.; Bluemel, A.; Gebhardt, S.; Quoc, T.V.; Dech, S. Remote sensing of mangrove ecosystems: A review. *Remote Sens.* **2011**, *3*, 878–928. [[CrossRef](#)]
17. Heumann, B.W. Satellite remote sensing of mangrove forests: Recent advances and future opportunities. *Prog. Phys. Geogr.* **2011**, *35*, 87–108. [[CrossRef](#)]
18. Leempoel, K.; Satyanarayana, B.; Bourgeois, C.; Zhang, J.; Chen, M.; Wang, J.; Bogaert, J.; Dahdouh-Guebas, F. Dynamics in mangroves assessed by high-resolution and multi-temporal satellite data: A case study in zhanjiang mangrove national nature reserve (zmnrr), PR China. *Biogeosciences* **2013**, *10*, 5681–5689. [[CrossRef](#)]
19. Wang, L.; Jia, M.; Yin, D.; Tian, J. A review of remote sensing for mangrove forests: 1956–2018. *Remote Sens. Environ.* **2019**, *231*, 111223. [[CrossRef](#)]
20. Lewis, R.R., 3rd; Milbrandt, E.C.; Brown, B.; Krauss, K.W.; Rovai, A.S.; Beever, J.W., 3rd; Flynn, L.L. Stress in mangrove forests: Early detection and preemptive rehabilitation are essential for future successful worldwide mangrove forest management. *Mar. Pollut. Bull.* **2016**, *109*, 764–771. [[CrossRef](#)]
21. Tian, B.; Wu, W.; Yang, Z.; Zhou, Y. Drivers, trends, and potential impacts of long-term coastal reclamation in China from 1985 to 2010. *Estuar. Coast. Shelf Sci.* **2016**, *170*, 83–90. [[CrossRef](#)]
22. Fu, H.; Liu, X.; Sun, Y. Application of RS in Wetland Ecosystem Health Assessment: A Case Study of Dagu River Estuary. In Proceedings of the 2008 International Workshop on Education Technology and Training & 2008 International Workshop on Geoscience and Remote Sensing, Shanghai, China, 21–22 December 2008; pp. 279–282.
23. Nittrouer, C.A.; Mullarney, J.C.; Allison, M.A.; Ogston, A.S. Sedimentary processes building a tropical delta yesterday, today, and tomorrow: The mekong system. *Oceanography* **2017**, *30*, 10–21. [[CrossRef](#)]
24. Willemsen, P.W.J.M.; Horstman, E.M.; Borsje, B.W.; Friess, D.A.; Dohmen-Janssen, C.M. Sensitivity of the sediment trapping capacity of an estuarine mangrove forest. *Geomorphology* **2016**, *273*, 189–201. [[CrossRef](#)]
25. Jayanthi, M.; Thirumurthy, S.; Nagaraj, G.; Muralidhar, M.; Ravichandran, P. Spatial and temporal changes in mangrove cover across the protected and unprotected forests of India. *Estuar. Coast. Shelf Sci.* **2018**, *213*, 81–91. [[CrossRef](#)]
26. Kamal, M.; Phinn, S.; Johansen, K. Characterizing the spatial structure of mangrove features for optimizing image-based mangrove mapping. *Remote Sens.* **2014**, *6*, 984–1006. [[CrossRef](#)]
27. Li, Z.; Xie, C.; He, X.; Guo, H.; Wang, L. Dynamic changes of landscape pattern and vulnerability analysis in qingyi river basin. *IOP Conf. Ser. Earth Environ. Sci.* **2017**, *94*, 012189. [[CrossRef](#)]
28. Lin, Y.; Hu, X.; Zheng, X.; Hou, X.; Zhang, Z.; Zhou, X.; Qiu, R.; Lin, J. Spatial variations in the relationships between road network and landscape ecological risks in the highest forest coverage region of China. *Ecol. Indic.* **2019**, *96*, 392–403. [[CrossRef](#)]
29. Walters, B.B.; Rönnbäck, P.; Kovacs, J.M.; Crona, B.; Hussain, S.A.; Badola, R.; Primavera, J.H.; Barbier, E.; Dahdouh-Guebas, F. Ethnobiology, socio-economics and management of mangrove forests: A review. *Aquat. Bot.* **2008**, *89*, 220–236. [[CrossRef](#)]
30. Araújo, L.; Silva, M.F.S.; Gomes, D.d.N.; Sousa, M.B.; Mayo, S.J.; de Andrade, I.M. Structure of a disturbed mangrove in the Rio Parnaíba delta, Piauí, northeast Brazil. *Feddes Repert.* **2018**, *129*, 75–91. [[CrossRef](#)]
31. Holm, A.M.; Cridland, S.W.; Roderick, M.L. The use of time-integrated noaa ndvi data and rainfall to assess landscape degradation in the arid shrubland of western Australia. *Remote Sens. Environ.* **2003**, *85*, 145–158. [[CrossRef](#)]
32. Hill, M.J.; Donald, G.E. Estimating spatio-temporal patterns of agricultural productivity in fragmented landscapes using avhrr ndvi time-series. *Remote Sens. Environ.* **2003**, *84*, 367–384. [[CrossRef](#)]
33. Jia, M.; Wang, Z.; Wang, C.; Mao, D.; Zhang, Y. A new vegetation index to detect periodically submerged mangrove forest using single-tide sentinel-2 imagery. *Remote Sens.* **2019**, *11*, 2043. [[CrossRef](#)]
34. Wattayakorn, G. Environmental issues in the gulf of Thailand. In *The Environment in Asia Pacific Harbours*; Springer: Berlin/Heidelberg, Germany, 2006; pp. 249–259.
35. Sathirathai, S.; Barbier, E.B. Valuing mangrove conservation in southern Thailand. *Contemp. Econ. Policy* **2001**, *19*, 109–122. [[CrossRef](#)]

36. Davies, K.P.; Murphy, R.J.; Bruce, E. Detecting historical changes to vegetation in a cambodian protected area using the landsat tm and etm+ sensors. *Remote Sens. Environ.* **2016**, *187*, 332–344. [[CrossRef](#)]
37. USGS Landsat Collections. *Fact Sheet*; USGS, Ed.; USGS: Reston, VA, USA, 2018; p. 2.
38. Gorelick, N.; Hancher, M.; Dixon, M.; Ilyushchenko, S.; Thau, D.; Moore, R. Google earth engine: Planetary-scale geospatial analysis for everyone. *Remote Sens. Environ.* **2017**, *202*, 18–27. [[CrossRef](#)]
39. Farr, T.G.; Rosen, P.A.; Caro, E.; Crippen, R.; Duren, R.; Hensley, S.; Kobrick, M.; Paller, M.; Rodriguez, E.; Roth, L. The shuttle radar topography mission. *Rev. Geophys.* **2007**, *45*, 583–585. [[CrossRef](#)]
40. Potapov, P.; Tyukavina, A.; Turubanova, S.; Talero, Y.; Hernandez-Serna, A.; Hansen, M.; Saah, D.; Tenneson, K.; Poortinga, A.; Aekakkararungroj, A. Annual continuous fields of woody vegetation structure in the lower mekong region from 2000–2017 landsat time-series. *Remote Sens. Environ.* **2019**, *232*, 111278. [[CrossRef](#)]
41. Giri, C.; Ochieng, E.; Tieszen, L.L.; Zhu, Z.; Singh, A.; Loveland, T.; Masek, J.; Duke, N. *Global Mangrove Forests Distribution, 2000*; NASA Socioeconomic Data and Applications Center (SEDAC): Palisades, NY, USA, 2013.
42. Jayanthi, M.; Thirumurthy, S.; Samynathan, M.; Duraisamy, M.; Muralidhar, M.; Ashokkumar, J.; Vijayan, K.K. Shoreline change and potential sea level rise impacts in a climate hazardous location in southeast coast of India. *Environ. Monit. Assess.* **2018**, *190*, 51. [[CrossRef](#)]
43. Tran Thi, V.; Tien Thi Xuan, A.; Phan Nguyen, H.; Dahdouh-Guebas, F.; Koedam, N. Application of remote sensing and gis for detection of long-term mangrove shoreline changes in Mui Ca Mau, Vietnam. *Biogeosciences* **2014**, *11*, 3781–3795. [[CrossRef](#)]
44. Ding, Z.; Liao, X.; Su, F.; Fu, D. Mining coastal land use sequential pattern and its land use associations based on association rule mining. *Remote Sens.* **2017**, *9*, 116. [[CrossRef](#)]
45. White, J.C.; Wulder, M.A.; Hermosilla, T.; Coops, N.C.; Hobart, G.W. A nationwide annual characterization of 25 years of forest disturbance and recovery for canada using landsat time-series. *Remote Sens. Environ.* **2017**, *194*, 303–321. [[CrossRef](#)]
46. Stephen, M.; Gu, C.; Yang, H. Visibility graph based time-series analysis. *PLoS ONE* **2015**, *10*, e0143015. [[CrossRef](#)] [[PubMed](#)]
47. Cleveland, W.S.; Devlin, S.J. Locally weighted regression: An approach to regression analysis by local fitting. *J. Am. Stat. Assoc.* **1988**, *83*, 596–610. [[CrossRef](#)]
48. Noether, G.E. Why kendall tau? *Teach. Stat.* **1981**, *3*, 41–43. [[CrossRef](#)]
49. Croux, C.; Dehon, C. Influence functions of the spearman and kendall correlation measures. *Stat. Methods Appl.* **2010**, *19*, 497–515. [[CrossRef](#)]
50. Krauss, K.W.; Lovelock, C.E.; McKee, K.L.; López-Hoffman, L.; Ewe, S.M.; Sousa, W.P. Environmental drivers in mangrove establishment and early development: A review. *Aquat. Bot.* **2008**, *89*, 105–127. [[CrossRef](#)]

